Vol.30 No.2 Nov 2019

NEWSLETTER ATMOSPHERIC ELECTRICITY

A photo captured at the Tall-Object Lightning Observatory in Guangzhou (TOLOG) on May 6, 2016 using a Nikon D7000 DSLR with an exposure time of 1 s

INTERNATIONAL COMMISSION ON ATMOSPHERIC ELECTRICITY
IAMAS IUGG
ICAE

http://www.icae-iamas.org

First announcement of the Workshop 'Radio Observations and Theory of Atmospheric Discharge Processes'

Bath UK, from Jun 29 - Jul 3, 2020

The main aim of the workshop is to stir in-depth discussions on all aspects of observations and theory of atmospheric discharges to identify critical open questions and promising future developments to advance the field. Potential topics include, but are not limited to, interferometry, sferics, radio signatures, lightning initiation and propagation, high energy atmospheric physics, general electrical discharges, streamers, leaders, and the lightning impact on the mesosphere and ionosphere. Contributions that combine observations with theory are particularly welcome.

Tentative program:

* Radio observations / interferometry & sferics
* High energy atmospheric physics - radio signatures & discharge theory
* Lightning effects on the upper atmosphere / mesosphere & ionosphere
* Physical mechanisms of discharge processes / streamers & leaders
* Lightning discharges / physics & effects

Invited Speakers:

Alejandro Luque, Caitano da Silva, Joseph Dwyer, Maribeth Stolzenburg, Martin Fullekrug, Michael Briggs, Michael Stock, Mitsuteru Sato, Morris Cohen, Nikolai Ostgaard, Ninyu Liu, Olaf Scholten, Paul Krehbiel, Phil Bitzer, Robert Marshall, Robert Moore, Sebastien Celestin, Steven Cummer, Thomas Marshall, Torsten Neubert, Ute Ebert, Victor Pasko, Vladimir Rakov, Xiushu Qie, Xuan-Min Shao.

The workshop will take place from Jun 29-Jul 3, 2020, at the University of Bath in Southwest England. Bath is a UNESCO world heritage site and a treat to visit as the second most important tourist attraction after London. The attendance of the workshop is free of any charges - complimentary coffee/tea will be served, but there are no additional resources available to us to cover your travel expenses.

The deadline for registration for contributed presentations is **March 29th, 2020**, such that there is good time to prepare an engaging program of activities. If you are planning to attend, it is recommended to book accommodation as early as possible, as June is a busy time for tourism in Bath.

If you are interested to attend the workshop, please register here:
https://www.ctrwiae.org/workshop2020_

You may find these links helpful to plan your travel:
How to get to Bath: https://www.ctrwiae.org/howtogettobath
Where to stay in Bath: https://www.ctrwiae.org/accommodationinbath
How to get to the University of Bath: https://www.ctrwiae.org/howtogettobathuniversity

Many thanks for your consideration and we look forward meeting up with you near soon.

The organizing committee
Joe Dwyer, Martin Fullekrug, Ningyu Liu, Steve Cummer

The EGU General Assembly 2020

The EGU General Assembly 2020, will take place in Vienna (Austria) on 3–8 May 2020, and will bring together geoscientists from all over the world to one meeting covering all disciplines of the Earth, planetary, and space sciences. Following the successful sessions at last year's conference, the convernors wish to invite you to submit abstracts to the Session NH1.3: "Atmospheric Electricity, Thunderstorms, Lightning and their effects".

Convernors: Yoav Yair, Sonja Behnke, Martino Marisaldi, Keri Nicoll and Serge Soula

Session description is to be found at:
https://meetingorganizer.copernicus.org/EGU2020/sessionprogramme#NH1

The deadline for abstract submission is **15 January 2020, 13:00 CET**. Please go to "Abstract Submission" and use your Copernicus user name and password.

The JpGU-AGU annual meeting

The joint JpGU-AGU annual meeting, will be held in Chiba, Tokyo on May 24-28th 2020. More information can be found at: http://www.jpgu.org/meeting_e2020/program.php. Please consider submitting to the session **"Effects of lightning, severe weather and tropical storms"**.

Chairs: Mitsutero Sato;

Co-Chairs: Yukihiro Takahashi, Yoav Yair, Xiushu Qie

The session invites contributions dealing with thunderstorms and lightning and their atmospheric effects with focusing on convective storm evolution, forecasting of thunderstorms and lightning using regional and global detection networks as well as other sensors. Also, works on global lightning patterns in an era of climate change, satellite-based studies of thunderstorms and other remote-sensing technologies, as well as urban effects on lightning and public safety from lightning danger. These will be international sessions, held in English; 125 M-SD. Two oral slots have been allocated in the preliminary program.

Abstract submission times will be from **January 7th through February 18th, 2020.**

Mark your calendars accordingly!

The 35th International Conference on Lightning Protection

The 35th International Conference on Lightning Protection (ICLP) will be held at the Shangri La Hotel, in Colombo, Sri Lanka 30th August to 4th September 2020.

Conference topics:

- Lightning Physics and phenomenology
- Lightning discharge
- Lightning occurrence characteristics
- Lightning attachment
- Lightning electromagnetic impulse (LEMP) and lightning-induced effects
- Lightning down-conductors and grounding
- Lightning protection of transportation systems
- Lightning protection of telecommunication systems
- Lightning protection of power systems
- Lightning protection of electronic systems
- Lightning protection of buildings
- Lightning protection of renewable energy systems
- Practical lightning protection
- Lightning protection and lightning testing standards
- Lightning safety, medicine and education
- High-voltage/triggered lightning experiments for simulation of lightning effects
- Special session on lightning protection of railway systems

This is a reminder that the paper submission deadline is **February 29th, 2020**. Your contribution is important for the success of the conference! You are encouraged to visit the conference website http://iclp2020.org/.

ICLP2020 Local organizing committee

Atmospheric Electricity Group – INPE

On the Triggering Mechanisms of Upward Lightning. We are now preparing the next summer and will be looking for attachment processes to common buildings and short towers inside and nearby INPE facilities in S. Paulo/Brazil. We will also measure X-rays emissions from leaders (Figure 1).

High-speed video observation of a dart leader producing x-rays. It was known that lightning can produce x-rays. However, in this study, thanks to the use of a high-speed video camera it was possible to determine when lightning produces x-rays, how far it was, how it was oriented when the detection of x-rays, and what the conditions of the pre-existing channel were during the leader propagation. The observations of the present work allow for new insights, confirmation of some hypotheses and comparison with past studies. The results presented help to understand why x-rays are sometimes detected and sometimes not. It is shown that the amount of charge transferred by the discharge plays a crucial role. This study also confirms that the orientation of the descending leader plays an important role in the detection of x-rays (Figure 2).

Figure 1 Triggering flash components that cause the upward leader initiation.

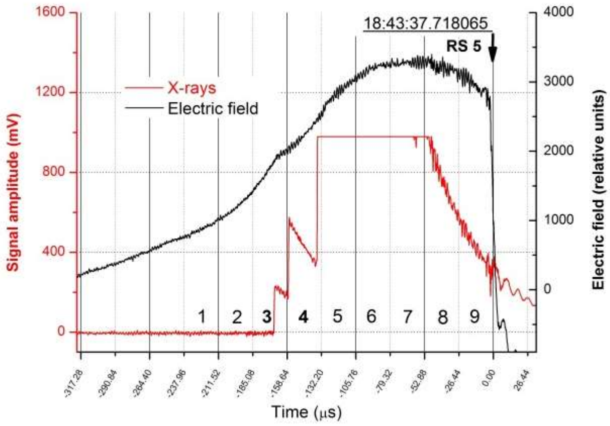

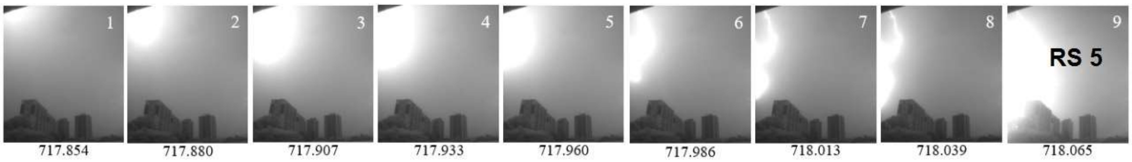

Figure 2 Plot of X-rays, E-field and high-speed camera images of a dart leader that produced X-rays.

Institute of Atmospheric Physics, Chinese Academy of Sciences (IAP, CAS), Beijing, China

Circuitous attachment in altitude triggered lightning. The attachment process with circuitous "S" shaped route in altitude triggered lightning striking a 30-m tower was observed between the lower extremity of the triggering wire and the upper tip of the tower in SHATLE. The downward negative leader from the triggering wire and the upward connecting positive leader from the tower tip "missed" with each other for a vertical distance of 4.1 m, then both turned horizontal and eventually connected during the breakdown through phase, with a total channel length of 25.3 m, close to a factor of 2 of the direct distance (13 m) between the wire tip and tower tip. This attachment process produced a sharp current pulse with duration of 19 μs and peak of 11.6 kA. The first 8 return strokes of the lightning developed through the "S" shape channel while the last one altered the attachment route by directly bridging the gap from the wire tip and the tower tip, which may be caused by the long interstroke interval facilitating the channel cooling and the conductivity decreasing (Figure 1).

Intermittent propagation of upward positive leader connecting a downward negative leader in a negative cloud-to-ground lightning. Both upward positive connecting leader (UPL) and downward negative leader (DNL) involved in a lightning striking the 325-m meteorology tower were captured by using a high-speed video camera with 2.7 μs time-resolution and 1 m spatial-resolution, and electromagnetic field measurements. The two exhibited different intermittent feature with temporal-inconsistent steps, suggesting that their stepping were independent from each other. When the DNL was very close to the UPL, the DNL can induce and support the UPL development via enhancing the overall electric field. It seems that the generation of space stems and their bridging to the DNL, as involved in the DNL stepping, might not the direct cause of the UPL intermittence.

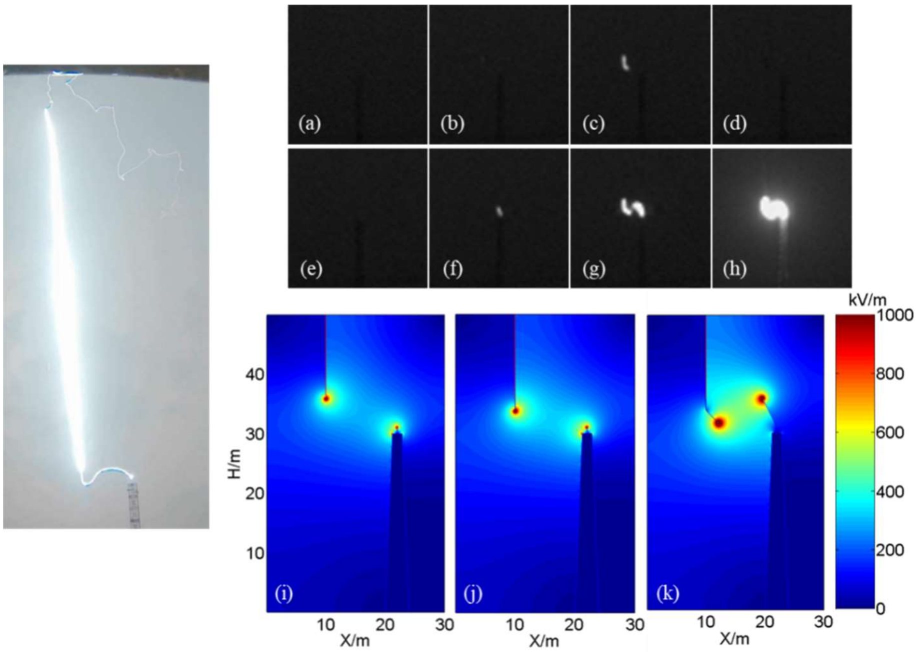

Figure 1 (left) still photograph of the circuitously attached discharge to the tower, (a)~(h) high speed video frames of the leader behaviors for the attachment, and (i)~(k) simulated electrostatic field at three instants for initiation and attachment of leaders.

Characteristics of impulsive currents superimposing on continuous/continuing current of rocket-triggered lightning. Characteristics and mechanism of initial continuous current (ICC) pulses and M components in rocket-triggered lightning are investigated. In two special cases, there are multiple current surges superimposed on the extremely long lasting ICC and continuing current (CC), which serve to keep the grounding channel active and extend the channel network inside the cloud, and hence prolong the ICC/CC duration. This situation reduced the possibility of RSs thereafter. By checking the in-cloud discharge behaviours based on the VHF radiation source mapping, ground E-field changes and the simutaneous current data, a new scenario leading to M-component was identified. It involves a short-term interruption of the upward RS wave (or weakening of breakdown through the main channel) and then a reactivation of the breakdown as promoted by the residual charge (Ma et al., 2019, IEEE TEMC).

Comparative study on the lightning sferics associated with terrestrial gamma-ray flashes observed in Americas and Asia. The broadband (< 1 Hz to 400 kHz) electromagnetic lightning signals associated with terrestrial gamma-ray flashes (TGFs) observed in America and Asia that detected by RHESSI and Fermi during 2010/2011 are compared. The general features of TGF-associated lightning sferics are consistent with previous findings that gamma-rays in TGFs are typically produced during a slow process that creates a considerable (but not necessarily) charge moment change within several milliseconds. The gamma-ray production is connected to a major fast discharge early in this slow process. Till now, the comprehensive data of more TGFs in South China have been collected and detailed analysis is under way (Lu et al., 2019, JASTP).

First positive polarity gigantic jet recorded near the Yellow Sea in mainland China. The first +GJ was recorded at 12:16:22 UTC on 12 August 2010, with the top altitude about 89 km. The parent thunderstorm formed in a very moist environment with moderate convective available potential energy (1294 J/kg) and lifted index (-3.19), and strong 0-6 km wind speed shear (16.3 m/s), that are not much different from typical summer thunderstorms. The south cell of the storm featured overshooting top around the time of the GJ. The storm was dominated by -CG flashes with an increase in -CG flash rate around the time of the GJ occurrence, indicating the storm appeared to be of normal polarity. The +GJ analyzed in this paper contributes to a growing population of observations of this rare phenomenon (He et al., 2019, JASTP).

Red Sprite in Southern Tibetan Plateau observed by ISUAL. The sprite phenomenon over southern foot of Tibet Plateau is examined by comparing the lightning detection data from WWLLN and the observation from ISUAL aboard the FORMOSAT-2 satellite. Most of the location accuracy of ISUAL is good after analyzing 17 cases and the deviations from WWLLN are less than 50 km. Based on this situation, the characteristics of parent lightning strokes of sprite are analyzed combining with the cloud-top brightness temperature data from FY 2 satellite. It was found that not only mesoscale convective system, but also the small scale convective system can bring sprites on southern Tibetan Plateau.

Potential effects of aerosol on lightning activity in Beijing metropolitan region. Beijing Lightning NETwork (BLNET) is a regional total-flashes three-dimension location network. The sensors, network layout and location algorithm were gradually updated to improve the performance of BLNET. Based on the lightning data from BLNET and PM2.5 data from 35 automatic air-monitoring stations, the response of lightning activities to aerosols is investigated for 117 thunderstorm days. The peak lightning activity under relatively polluted condition occurred 4 hours later than that under relatively clean condition, enhancing the percentage of total flashes by a factor of ~2. A significant positive correlation was found when PM2.5 lower than 130 μg•m^{-3}. On the contrary, as PM2.5 exceeded 150 μg•m^{-3}, total flashes showed a negative relationship to PM2.5. When PM2.5 ranged from 130 to 150 μg•m^{-3}, the relationship between aerosols and lightning was very weak.

Lightning jumps in hailfall nowcasting in the Beijing area. Based on total lightning data from BLNET, hailfall reports from 2015 to 2017 in Beijing, and S-band radar data from Beijing Meteorological Observation Center, the total lightning activities for 148 hailfall events are analyzed with the identification method of strong convective cells (CCs). Most of the hailstorms have a very high flash rate (FR), and a significant increase in FR is observed before hailfall events. The average lightning jump (LJ) lead time is 27.1 min. LJs precede 81.8% of all hailfall events, and 38.6% of LJs are not followed by hailfall reports within one hour. Most hailfall events occurred at the boundary of strong CCs instead of the cell centers. This study shows that the total LJ is a potentially useful predictor for hail nowcasts in the Beijing area (Tian et al., 2019, AR).

Laboratory of Lightning Physics and Protection Engineering (LiP&P), State Key Laboratory of Severe Weather (LASW), Chinese Academy of Meteorological Sciences (CAMS), Beijing, China

High-Speed Video Observations of Recoil Leaders Producing and Not Producing Return Strokes in a Canton-Tower Upward Flash. High-speed video and electric field change data have been used to examine the initiation and propagation of 21 recoil leaders, 7 of which evolved into dart (or dart-stepped) leaders (DLs) initiating return strokes and 14 were attempted leaders (ALs), in a Canton-Tower upward flash. Three DLs and two ALs clearly exhibited bidirectional extension. Each DL was preceded by one or more ALs and initiated near the extremity of the positive end of the preceding AL. The negative end of each bidirectional DL extended along one of the decayed branches of the flash-initiating upward positive leader, attached to the top of the Canton Tower, and initiated a return stroke. In contrast, the positive end of each bidirectional DL generally appeared to be inactive (stationary) or intermittently propagated along the positive part of the preceding AL channel and extended into the virgin air. A sequence of two floating channel segments was formed ahead of the approaching positive end of one DL, causing its abrupt elongation.

Initial leader properties during the preliminary breakdown processes of

lightning flashes and their associations with initiation positions. The properties of initial leaders (ILs) of 1,056 flashes in two thunderstorms in Guangzhou, China, are analyzed. The median values of IL properties are 11.1 ms for duration, 2.2 km for vertical distance, 2.7 km for 3-D distance, 1.9×10^5 m/s for vertical displacement speed, 2.4×10^5 m/s for 3-D displacement speed, 28° for angle between the IL's displacement direction and the vertical direction, 1.1 per ms for pulse rate, 179 m for vertical step length, and 224 m for 3-D step length. All the IL properties follow lognormal distributions. Strong monotonic relationships of IL duration with speed and pulse rate and pulse rate with speed and step length are revealed. With increasing initiation altitude, IL duration and step length tend to increase, and IL speed and pulse rate tend to decrease. It is further speculated that the difference between the IL durations and pulse rates of CG lightning and IC lightning indicated by previous studies may be essentially associated with the difference in their predominant initiation altitudes. The ILs initiated at approximately the −20 °C isotherm are more vertically orientated on average than those initiated at lower or higher levels. The ILs initiated in the strong kinematic areas generally have a greater speed and pulse rate but smaller duration, distance, and step length relative to those initiated in the weak kinematic areas. The different electric field intensity predominantly impacted by the charge densities in strong and weak kinematic areas is suggested to be responsible for this comparison. By comparing the IL properties in the normal thunderstorms in this study and those in supercells reported by Zheng et al. (2018), it is proposed that the differences of kinematics and charge structures between these two types of thunderstorms should be responsible for their distinct IL properties. Charge distribution pattern plays a more important role in a severe thunderstorm in determining the ambient electric field and then the IL properties in different storm regions, whereas the more important factor for a normal thunderstorm is the charge density.

Numerical Simulation of the Formation of a Large Lower Positive Charge Center in a Tibetan Plateau Thunderstorm. Numerical modeling is applied to elucidate the formation mechanism of the large lower positive charge centers (LPCCs) observed during thunderstorms over the Tibetan Plateau based on the simulation of a storm at the northeastern boundary of the plateau. Four sensitivity tests were carried out to explore the impacts of inductive charging, reversal temperature, and the choice of non-inductive charging scheme. The results show that the unique environmental conditions of the Qinghai-Tibet Plateau, which include weak convection and low freezing level, are fundamental to the formation of large LPCC. A weakened charge density in the upper positive charge center (UPCC) highlights the role of a LPCC in lightning initiation although the charge density of the LPCC has no obvious change compared to that in the LPCC of the typical tripole structure. This accounts for Tibetan Plateau thunderstorms having low frequencies of lightning flashes, which occur mainly in the lower dipole. Inductive electrification, which provided more than 50% of the positive charge on graupel and increased the positive and negative charge on cloud drops by two orders of magnitude, is an important complement to the lower dipole of the tripole charge structure originally established by non-inductive electrification (Figure 1). The inductive electrification also evidently enhances the LPCC and the middle negative charge center, while slightly reducing the UPCC. Subsequently, the lightning activity is strengthened, and lightning flashes are more likely to be initiated at the lower dipole. Varying the reversal temperatures and non-inductive charging scheme does not fundamentally affect the formation of the LPCC.

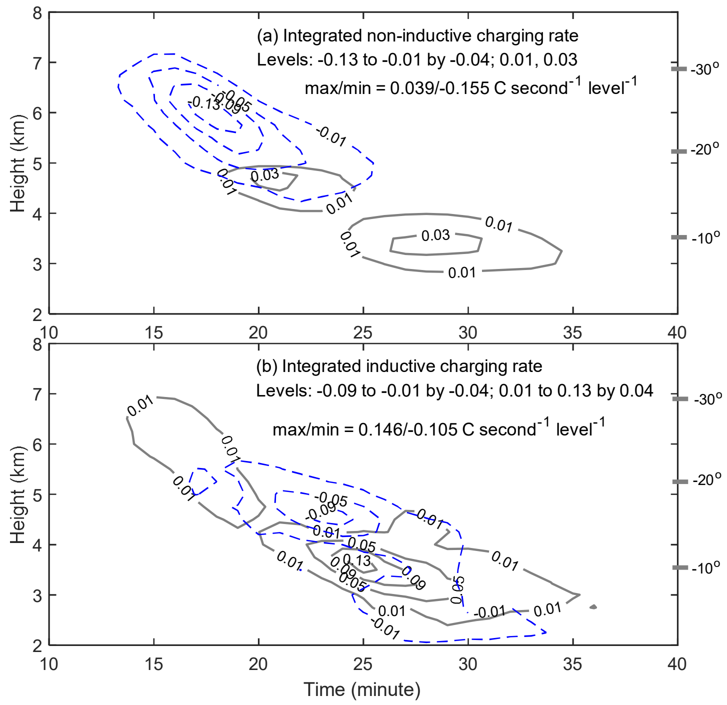

Figure 1 (a) Non-inductive and (b) inductive charging rates, integrated by model level (250 m thickness), between graupel and ice crystals. Gray lines and blue dashed lines indicate the positive and negative charges obtained by graupel through the charging process, respectively.

High-speed video observations of natural lightning attachment process with framing rates up to half a million frames per second. Using high-speed video cameras operating with framing rates of 20 and 525 kiloframes per second, we imaged the attachment process of a natural negative cloud-to-ground flash, occurring at a distance of 490 m. Nine upward leaders were observed. A total of 12 space stems/leaders in 47 steps of the downward negative stepped leader were captured. The 2D length of them was between 2.0 and 5.9 m, with an average of 3.0 m. The average interstep interval, step length, and two-dimensional speed of the downward negative leader and that of upward positive leader were statistically analyzed. The last step of the downward negative leader making contact with the upward connecting leader was recorded. The two-dimensional length of the final imaged gap between the tips of opposite-polarity leaders was estimated to be about 13 m. The Sequential images, captured by high-speed video camera HC-4, are shown in Figure 2.

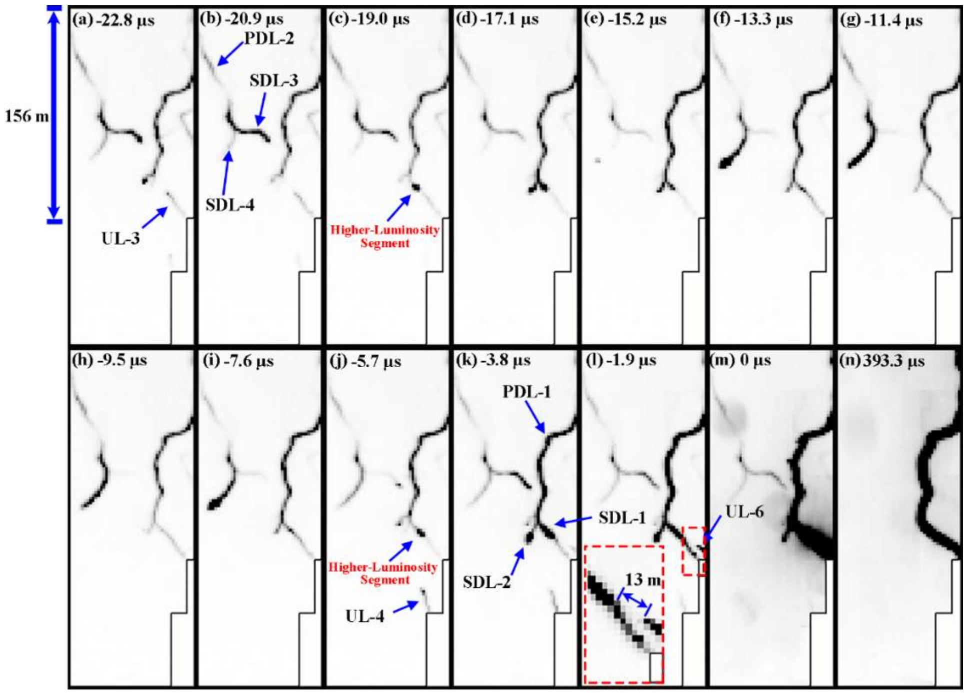

Figure 2 (a) to (m) Sequential images captured by high-speed video camera HC-4 (525 kfps) of the flash from -22.8 to 0 μs before and during the first return stroke onset and (n) the stroke channel 393.3 μs after the return-stroke onset. The images were inverted and contrast enhanced. Two primary branches of downward leader (PDL-1 and PDL-2), four secondary branches of downward leaders (SDL1-4), three ULs (UL-3, UL-4, UL-6), and two higher-luminosity segments are labeled. The area in dashed-line box in (l) is shown enlarged in the lower-left. The contours of buildings B2 and B3 are shown in the lower-right corner of each frame. It is not clear if the higher-luminosity segment seen in (j) was formed in virgin air or along the remnants of UL-3. The latter was competing for interception of SDL-1 with UL-6, but apparently lost.

Lightning Research Group of Gifu University (Gifu, Japan)

Temporal and Spatial Characteristics of Preliminary Breakdown Pulses in Intracloud Lightning Flashes. The preliminary breakdown (PB) process can radiate ample electromagnetic signals, as evidenced by the small- and large-amplitude pulses in the E-change waveforms. The overall locations of these pulses indicate that the PB processes in the normal IC flashes usually exhibit an obvious upward progression. So, does each PB pulse correspond to an advancing (upward) progression? Using 32 normal intracloud (IC) flashes recorded by a fast antenna lightning mapping array system called FALMA, we have studied the temporal and spatial characteristics of PB pulses. It was found that PB processes started with a stage of preliminary isolated pulses (PIPs), and followed by classic PB pulse (PBP) clusters. A typical PBP cluster consists of several narrow pulses (NPs) and one classic PBP. During one PIP stage, the pulses occurring later usually have a lower altitude, indicating a kind of backward extension relative to the overall upward progression of PB process. In each PBP cluster, PBP is always located at the lowest height and behind its preceding NPs. Based on the temporal and spatial characteristics of PB pulses, we have proposed a model shown in Figure 1 to interpret how the PIPs, NPs and PBPs are produced. The detailed information can be found in the paper *Temporal and Spatial Characteristics of Preliminary Breakdown Pulses in Intracloud Lightning Flashes* published in JGR.

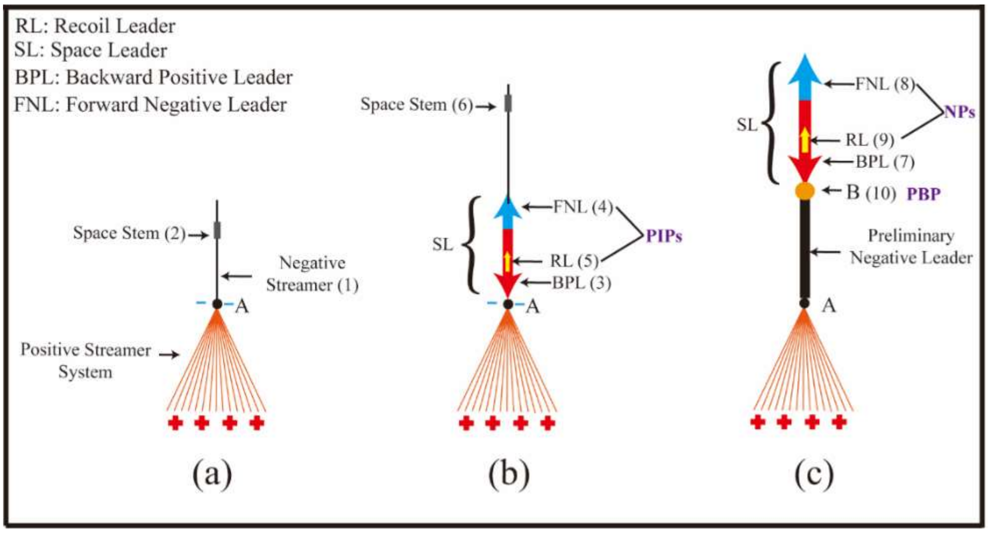

Figure 1 Illustration of the formation of PIPs, NPs, and PBPs in the PB process.

Multi-Termination CG Flashes observed by the FALMA. It has been clear that a significant fraction of negative cloud-to-ground (CG) lightning flashes strike the ground in two or more places. We call such a CG flash as multiple-termination flashes (MTFs). In this study, we have characterized 205 MTFs that were well imaged by the Fast Antenna Lightning Mapping Array (FALMA) in Japan during the summer of 2017. Figure 2 presents an example of the identified MTF that had seven return strokes (RSs) and two ground terminations. This flash started at a height of about 9 km above the sea level. From the pulse locations shown in Figure 2c, 2d, 2e and 2f, the first stroke terminated at one place marked by a triangle and the remaining 6 strokes terminated at another place marked by a square. There is a horizontal distance of about 6 km between the two termination points. As seen in Figure 2c, the leaders leading to the two terminations forked at a height of about 7 km. The detailed parameter statistics of 205 MTFs can be seen in the published paper *Characterization of Multi-Termination CG Flashes Using a 3D Lightning Mapping System FALMA*.

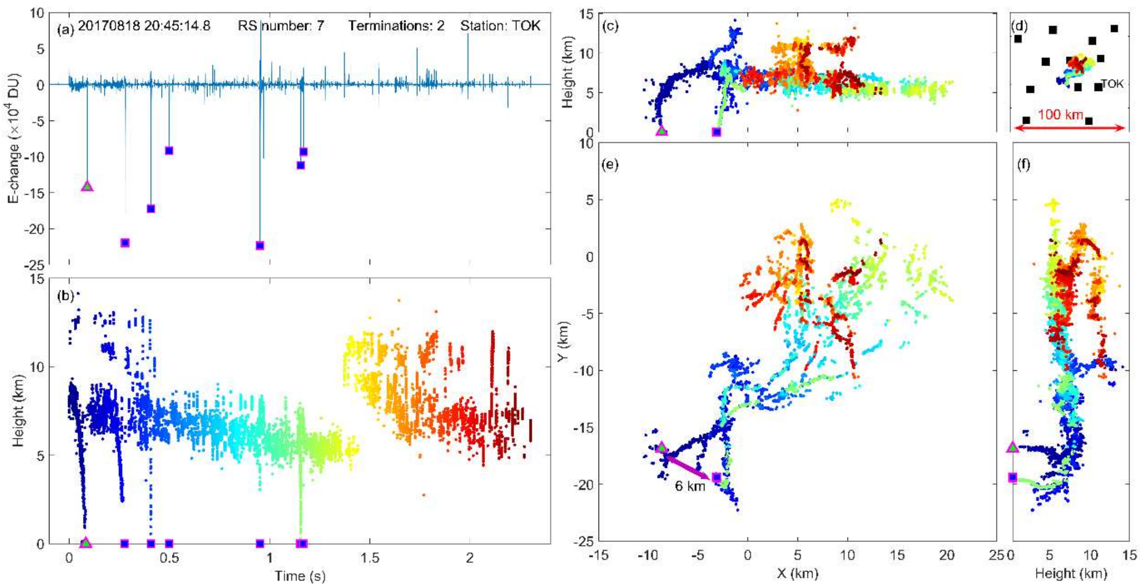

Figure 2 An example of negative CG lightning with two terminations. (a) E-change waveform recorded at the station TOK. The triangle and squares indicate the identified RSs. The abbreviation of DU stands for digital unit. (b) Pulse located height with time. (c) x-z vertical view. (d) Geographical positions of FALMA stations. (e) x-y view. (f) y-z vertical view.

Winter Lightning Observations with the FALMA. A FALMA system consisting of 14 sites was set up in the Hokuriku region from December 2018 to March 2019 for winter lightning observation. Preliminary analysis of the data showed that winter lightning flashes are generally very complicated. While lightning flashes in summer usually show well-defined basic structures of IC or -CG flashes, lightning flashes in winter usually do not show such simple structures. One example is shown in Figure 3. We can see that this flash started with normal IC discharges. The negative leader developed to a lower layer at about 800 ms and followed by 10 return strokes with two different terminations. An upward negative leader was detected right before the last return stroke. The animation of this flash can be found at http://tingwu.info/falma/ICAE2019_2.mp4.

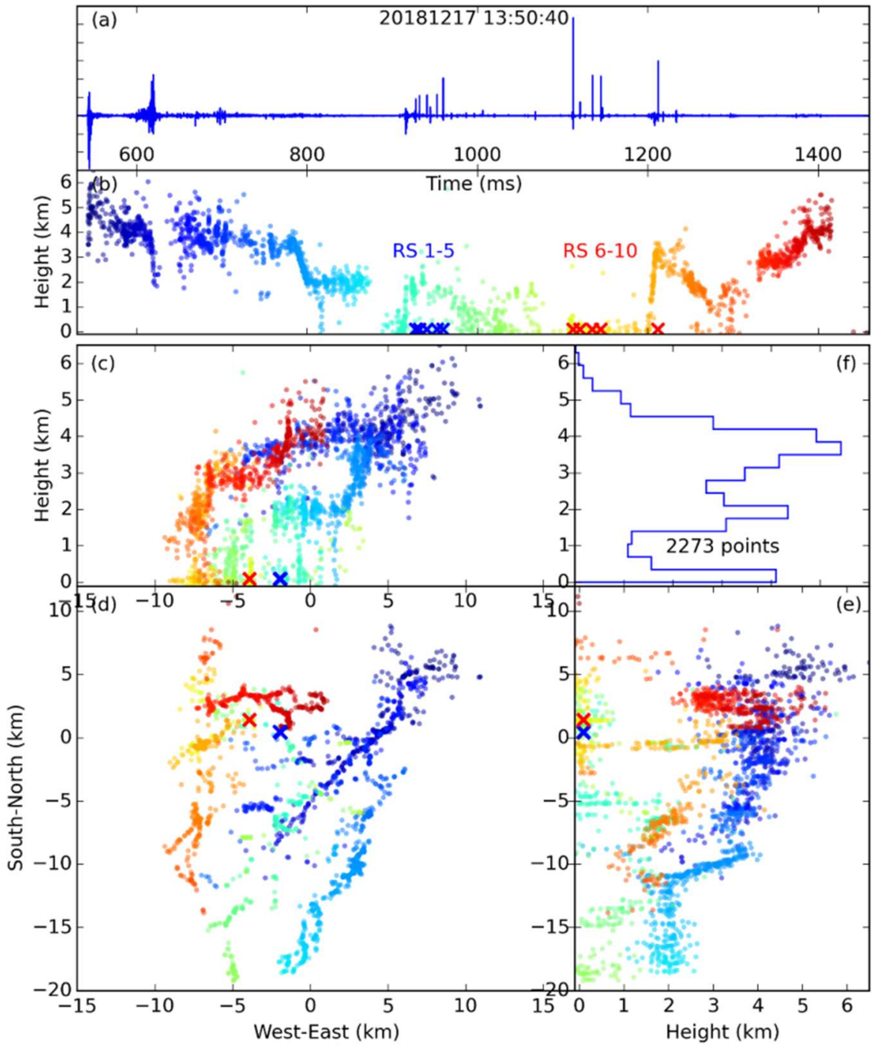

Figure 3 A complicated lightning flash in winter.

University of Florida (Gainesville, FL, USA)

A.F.R. Leal (Federal University of Para (UFPA), Belém, Brazil) and V.A. Rakov authored a paper titled “A study of the context in which compact intracloud discharges occur”. The occurrence context of compact intracloud discharges (CIDs) was examined using their electric field waveforms and corresponding NLDN data. A total of 1096 CIDs transporting negative charge upward and 8 CIDs transporting positive charge upward were analyzed. The CIDs were categorized based on whether they were isolated or were followed, preceded, or both followed and preceded by other NLDN-reported lightning events. The percentages of isolated CIDs transporting negative charge upward (lower-level CIDs) decreased from 92% for 5 km search radius and ±10 ms time window to 31% for 10 km and ±1000 ms, this decrease being accompanied by an increase of the percentage of CIDs preceding (initiating) normal lightning events from 6.8% to 43%. Other lower-level CID occurrence contexts were relatively rare. For the apparently most reasonable 10-km search radius and ±500 ms time window, 46% of lower-level CIDs were isolated and 37% appeared to initiate normal lightning events. For the latter CID category, normal lightning events mostly occurred within 2-km radius and less than 100 ms after the CID. Geometric mean (GM) NLDN-reported peak currents for isolated CIDs (33 kA) were similar to those initiating normal lightning events (34 kA). Some of the isolated CIDs could be viewed as precursors, because they apparently initiated normal lightning events at essentially the same location after time intervals measured in seconds. Lower-level CIDs whose electric field waveforms exhibited periodic variations (ringing) on the opposite-polarity overshoot were mostly isolated, while those without ringing in the electric field waveforms tended to initiate normal lightning events. CIDs transporting positive charge upward (upper-level CIDs) occurred at heights ranging from 16 to 19 km vs. 6 to 16 km for CIDs transporting negative charge upward (lower-level CIDs). GM value of NLDN-reported peak current for 8 upper-level CIDs was 113 kA vs. 33 kA for 1096 lower-level CIDs. The paper is published in the Springer Nature Scientific Reports.

M. D. Tran, I. Kereszy, V.A. Rakov, and J.R. Dwyer (University of New Hampshire, Durham, NH) authored a paper titled “On the Role of Reduced Air Density along the Lightning Leader Path to Ground in Increasing X-Ray Production Relative to Normal Atmospheric Conditions”. Cloud-to-ground lightning flashes are each typically composed of 3 to 5 strokes. First stroke necessarily develops in virgin (cold) air, while subsequent strokes often retrace the remnants of the channel(s) of preceding stroke(s). Lightning is known to produce hard X-rays during the initial (leader) stage of each of its strokes. Traditionally, first-stroke leaders were thought to be the main producers of X-rays, and subsequent-stroke leaders (developing in warm, low-density air) were thought to be less active X-ray producers. Mallick et al. (2012) observed subsequent-stroke leaders that were more prolific producers of X-rays than the first-stroke leader in the same flash. However, they had no high-speed video images to confirm that their subsequent leaders followed the same path to ground as the first leader, as opposed to forging a new path to ground through cold air. Tran et al. presented new observations, including high-speed video images, showing that a second stroke produced more detectable X-ray pulses than the first stroke, with both strokes following the same channel to ground. Additionally, they presented data for a subsequent stroke from a different flash, which show the rarely observed occurrence of significant X-ray emission at the time of attachment of that stroke to the ground, whereas there were no detectable X-rays associated with negative leader steps. The paper is published in the Geophysical Research Letters.

This list of references is not exhaustive. It includes only papers published during the last six months provided by the authors or found from an on-line research in journal websites. Some references of papers very soon published have been provided by their authors and included in the list. The papers in review process, the papers from Proceedings of Conference are not included.

Attanasio, A., Krehbiel, P.R., da Silva, C.L. 2019. Griffiths and Phelps lightning initiation model, revisited. J. Geophys. Res. Atmos., 124(14), 8076-8094.

Baba Y., Rakov, V.A. 2019. "Application of the FDTD Method to Lightning Studies", in "Lightning Interaction with Power Systems", Vol. 2, Ch. 11, ed. A. Piantini, IET, London, pp. 393-424.

Bagheri, M., Dwyer, J., McConnell, M.L. 2019. On the linear polarization of TGFs and X-rays from natural and rocket-triggered lightning and its association with source geometry. J. Geophys. Res. Space Physics, DOI: 10.1029/2019JA026570.

Bandara, S., Marshall, T., Karunarathne, S., et al. 2019. Characterizing three types of negative narrow bipolar events in thunderstorms. Atmos. Res., 227, 263-279.

Barth, M.C., Rutledge, S.A., Brune, W.H., et al. 2019. Introduction to the Deep Convective Clouds and Chemistry (DC3) 2012 studies. J. Geophys. Res. Atmos., 124(14), 8095-8103.

Berge, N., Celestin, S. 2019. Constraining downward terrestrial gamma ray flashes using ground-based particle detector arrays. Geophys. Res. Lett., 46(14), 8424-8430.

Chen, A. B-C., Chen, H., Chuang, C-W, et al. 2019. On negative Sprites and the polarity paradox. Geophys. Res. Lett., 46(16), 9370-9378.

Chen, Z., Qie, X., Liu, D., et al. 2019. Lightning data assimilation with comprehensively nudging water contents at cloud-resolving scale using WRF model. Atmos. Res., 221, 72-87.

Chen, Z., Zhang, Y., Zheng, D., et al. 2019. A method of three-dimensional location for LFEDA combining the time of arrival method and the time reversal technique. J. Geophys. Res. Atmos., 124(12), 6484-6500.

Chilingarian, A., Khanikyants, Y., Rakov, V.A., et al. 2020. Termination of thunderstorm-related bursts of energetic radiation and particles by inverted-polarity intracloud and hybrid lightning discharges. Atmos. Res., 233, 2020, DOI: 10.1016/j.atmosres.2019.104713.

Cooray, V., Cooray, G., Rubinstein, M., et al. 2019. Generalized electric field equations of a time-varying current distribution based on the electromagnetic fields of moving and accelerating charges. Atmosphere, 10(7), 367, DOI: 10.3390/atmos10070367.

Czernecki, B., Taszarek, M., Marosz, M., et al. 2019. Application of machine learning to large hail prediction-The importance of radar reflectivity, lightning occurrence and convective parameters derived from ERA5. Atmos. Res., 227, 249-262.

da Silva, C.L., Sonnenfeld, R.G., Edens, H.E., et al. 2019. The plasma nature of lightning channels and the resulting nonlinear resistance. J. Geophys. Res. Atmos., 124(16), 9442-9463.

Davis, T.C., Rutledge, S.A., Fuchs, B.R. 2019. Lightning location, NOx production, and transport by anomalous and normal polarity thunderstorms. J. Geophys. Res. Atmos., 124(15), 8722-8742.

Fabro, F., Montanya, J., van der Velde, O.A., et al. 2019. On the TGF/lightning ratio asymmetry. J. Geophys. Res. Atmos., 124(12), 6518-6531.

Fan, Y., Lu, G., Li, X., et al. 2019. Measurements of magnetic pulse bursts during initial continuous current of negative rocket-triggered lightning. J. Geophys. Res. Atmos., DOI: 10.1029/2019JD031237.

Fullekrug, M., Nnadih, S., Soula, S., et al. 2019. Maximum sprite streamer luminosity near the stratopause. Geophys. Res. Lett., DOI: 10.1029/2019GL084331.

Gao, P., Wang, D., Shi, D., et al. 2019. Characterization of multitermination CG flashes using a 3D lightning mapping system (FALMA). Atmosphere, 10, 625.

Guo, Z., Li, Q., Bretas, A., et al. 2019. A simplified physical model of negative leader in long sparks. Electr. Pow. Syst. Res., 176, 105955, https://doi.org/10.1016/j.epsr.2019.105955.

He, L., Rachidi, F., Azadifar, M., et al. 2019. Electromagnetic fields associated with the M-component mode of charge transfer. J. Geophys. Res. Atmos., 124(13), 6791-6809.

He, Q., Yang, J., Lu, G., et al. 2019. Analysis of the first positive polarity gigantic jet recorded near the Yellow Sea in mainland China. J. Atmos. Sol.-Terr. Phy., 190, 6-15.

Holzworth, R.H., McCarthy, M.P., Brundell, J.B., et al. 2019. Global distribution of superbolts. J. Geophys. Res. Atmos., 124, 9996-10005.

Hu, J., Rosenfeld, D., Zrnic, D., et al. 2019. Tracking and characterization of convective cells through their maturation into stratiform storm elements using polarimetric radar and lightning detection. Atmos. Res., 226, 192-207.

Huang, H., Wang, D., Wu, T. et al. 2019. Progression features of dart leaders in natural negative cloud-to-ground lightning flashes. J. Geophys. Res. Atmos., 124, DOI: 10.1029/2019JD030990.

Karagiannidis, A., Lagouvardos, K., Lykoudis, S., et al. 2019. Modeling lightning density using cloud top parameters. Atmos. Res., 222, 163-171.

Larkey, R. K., Sample, J. G., Smith, D. M., et al. 2019. Evidence for extended charging periods prior to terrestrial gamma ray flashes. Geophys. Res. Lett., DOI:

10.1029/2019GL083827.

Lavigne, T., Liu, C., Liu, N. 2019. How does the trend in thunder days relate to the variation of lightning flash density? J. Geophys. Res. Atmos., 124(9), 4955-4974.

Leal, A., Rakov, V.A. 2019. A study of the context in which compact intracloud discharges occur. Sci. Rep., 9, 12218, DOI: 10.1038/s41598-019-48680-6.

Liu, G., Yuan, P., An, T., et al. 2019. Using saha-boltzmann plot to diagnose lightning return stroke channel temperature. J. Geophys. Res. Atmos., 124(8), 4689-4698.

Liu, N., Dwyer, J.R., Tilles, J.N., et al. 2019. Understanding the radio spectrum of thunderstorm narrow bipolar events. J. Geophys. Res. Atmos., 124, 10134-10153.

Lopez, J.A., Montanya, J., van der Velde, O.A. et al. 2019. Charge structure of two tropical thunderstorms in Colombia. J. Geophys. Res. Atmos., 124(10), 5503-5515.

Lorenz, R.D., Imai, M., Takahashi, Y., et al. 2019. Constraints on Venus lightning from Akatsuki's first 3 years in orbit. Geophys. Res. Lett., 46(14), 7955-7961.

Lu, G., Zhang, H., Cummer, S. A., et al. 2019. A comparative study on the lightning sferics associated with terrestrial gamma-ray flashes observed in North America and Asia, J. Atmos. Sol.-Terr. Phy., 183, 67-75.

Ma, Z., Jiang, R., Sun, Z., et al. 2019. Characteristics of impulsive currents superimposing on continuous/continuing current of rocket-triggered lightning. IEEE Transactions on Electromagnetic Compatibility, DOI: 10.1109/TEMC.2019.2924993.

Mailyan, B.G., Xu, W., Celestin, S., et al. 2019. Analysis of individual terrestrial gamma-ray flashes with lightning leader models and fermi gamma-ray burst monitor data. J. Geophys. Res. Space Physics, 124(8), 7170-7183.

Marchand, M., Hilburn, K., Miller, S. D. 2019. Geostationary lightning mapper and earth networks lightning detection over the contiguous United States and dependence on flash characteristics. J. Geophys. Res. Atmos., DOI: 10.1029/2019JD031039.

Marisaldi, M., Galli, M., Labanti, C., et al. 2019. On the high-energy spectral component and fine time structure of terrestrial gamma ray flashes. J. Geophys. Res. Atmos., 124(14), 7484- 7497.

Ostgaard, N., Christian, H.J., Grove, J.E., et al. 2019. Gamma ray glow observations at 20-km altitude. J. Geophys. Res. Atmos., 124(13), 7236-7254.

Peterson, M. 2019. Research Applications for the Geostationary Lightning Mapper operational lightning flash data product. J. Geophys. Res. Atmos., 124, 10205-10231.

Peterson, M. 2019. Using lightning flashes to image thunderclouds. J. Geophys. Res. Atmos., 124, 10175-10185.

Pu, Y., Cummer, S.A., Lyu, F., et al. 2019. Low frequency raio pulses produced by terrestrial gamma-ray flashes. Geophys. Res. Lett., 46(12), 6990-6997.

Qi, Q., Lyu, W., Ma, Y., et al. 2019. High-speed video observations of natural lightning attachment process with framing rates up to half a million frames per second. Geophys. Res. Lett., DOI: 10.1029/2019GL085072.

Qie, X., Zhang, Y. 2019. A review of atmospheric electricity research in china from 2011 to 2018. Adv. Atmos. Sci., 36(9), 994-1014.

Rakov, V.A. 2019. "Lightning Phenomenon and Parameters for Engineering Application", in "Lightning Interaction with Power Systems", Vol. 1, Ch. 2, ed. A. Piantini, IET, London, pp. 47-99.

Ren, H., Tian, Y., Lu, G., et al. 2019. Total lightning signatures of thunderstorms and lightning jumps in hailfall nowcasting in the Beijing area. Atmos. Res., 230, 104646, DOI: 10.1016/j.atmosres.2019.104646.

Rutjes, C., Ebert, U., Buitink, S., et al. 2019. Generation of seed electrons by extensive air showers, and the lightning inception problem including narrow bipolar events. J. Geophys. Res. Atmos., 124(13), 7255-7269.

Saba, M.M.F., Ferro, M.A.S., Cuadros, E.T., et al. 2019. High-speed video observation of a dart leader producing x-rays. J. Geophys. Res. Space Physics, 1, p. 2019JA027247.

Sabri, M.H.M., Ahmad, M.R., Esa, M.R.M., et al. 2019. Initial electric field changes of lightning flashes in tropical thunderstorms and their relationship to the lightning initiation mechanism. Atmos. Res., 226, 138-151.

Schumann, C., Saba, M.M.F., Warner, T.A., et al. 2019. On the triggering mechanisms of upward lightning. Sci. Rep., 9, 9576.

Shi, D., Wang, D., Wu, T., et al. 2019. Temporal and spatial characteristics of preliminary breakdown pulses in intracloud lightning flashes. J. Geophys. Res. Atmos., 124, https://doi.org/10.1029/2019JD031130.

Shi, Z., Li, L., Tan, Y., et al. 2019. A numerical study of aerosol effects on electrification with different intensity thunderclouds. Atmosphere, 10(9), 508, DOI: 10.3390/atmos10090508.

Soula, S., Georgis, J.-F., Salaun, D. 2019. Quantifying the effect of wind turbines on lightning location and characteristics. Atmos. Res., 221, 98-110.

Stern, S., Cimarelli, C., Gaudin, D., et al. 2019. Electrification of experimental volcanic jets with varying water content and temperature. Geophys. Res. Lett., DOI: 10.1029/2019GL084678.

Sun, J., Chai, J., Leng, L., et al. 2019. Analysis of lightning and precipitation activities in three severe convective events based on doppler radar and microwave radiometer over the central china region. Atmosphere, 10(6), 298, DOI: 10.3390/atmos10060298.

Tran, M.D., Kereszy, I., Rakov, V.A., et al. 2019.

On the role of reduced air density along the lightning leader path to ground in increasing x-ray production relative to normal atmospheric conditions. Geophys. Res. Lett., 46(15), 9252-9260.

Wang, F. Deng, X., Zhang, Y. et al. 2019. Numerical simulation of the formation of a large lower positive charge center in a Tibetan Plateau thunderstorm. J. Geophys. Res. Atmos., 124(16), 9561-9593.

Wu, B., Lyu, W., Qi, Q., et al. 2019. High-speed video observations of recoil leaders poducing and not producing return strokes in a canton-tower upward flash. Geophys. Res. Lett., 46, 8546–8553.

Wu, T., Wang, D., Takagi, N. 2019. Intracloud lightning flashes initiated at high altitudes and dominated by downward positive leaders. J. Geophys. Res. Atmos., 124(13), 6982-6998.

Wu, T., Wang, D., Takagi, N. 2019. Velocities of positive leaders in intracloud and negative cloud-to-ground lightning flashes. J. Geophys. Res. Atmos., 124, 9983-9995.

Xu, W., Celestin, S., Pasko, V.P., et al. 2019. Compton scattering effects on the spectral and temporal properties of terrestrial gamma-ray flashes. J. Geophys. Res. Space Physics, 124 (8), 7220-7230.

You, J., Zheng, D., Zhang, Y., et al. 2019. Duration, spatial size and radiance of lightning flashes over the Asia-Pacific region based on TRMM/LIS observations. Atmos. Res., 223, 98-113.

Zahlava, J., Nemec, F., Santolik, O., et al. 2019. Lightning, contribution to overall whistler mode wave intensities in the Plasmasphere. Geophys. Res. Lett., 46(15), 8607-8616.

Zhang, M., Yuan, P., Liu, G., et al. 2019. The current variation along the discharge channel in cloud-to-ground lightning. Atmos. Res., 225, 121-130.

Zhang, Y., Fan, Y., Jiang, R., et al. 2019. Examining the influence of current waveform on the lightning electromagnetic field at the altitude of halo formation, J. Atmos. Sol.-Terr. Phy., 189, 114-122.

Zheng, D., Shi, D., Zhang, Y., et al. 2019. Initial leader properties during the preliminary breakdown processes of lightning flashes and their associations with initiation positions. J. Geophys. Res. Atmos., 124(14), 8025-8042.

Zheng, D., Wang, D., Zhang, Y., et al. 2019. Charge regions indicated by LMA lightning flashes in Hokuriku's winter thunderstorms. J. Geophys. Res. Atmos., 124(13), 7179-7206.

Zhu, Y., Ding, Z., Rakov, V.A., et al. 2019. Evolution of an upward negative lightning flash triggered by a distant +CG from a 257-m-tall tower, including initiation of subsequent strokes. Geophys. Res. Lett., 46(12), 7015-7023.

NEWSLETTER
ATMOSPHERIC ELECTRICITY

REMINDER

Newsletter on Atmospheric Electricity presents twice a year (May and November) to the members of our community with the following information:

announcements concerning people from atmospheric electricity community, especially awards, new books...,

announcements about conferences, meetings, symposia, workshops in our field of interest,

brief synthetic reports about the research activities conducted by the various organizations working in atmospheric electricity throughout the world, and presented by the groups where this research is performed, and

a list of recent publications. In this last item will be listed the references of the papers published in our field of interest during the past six months by the research groups, or to be published very soon, that wish to release this information, but we do not include the contributions in the proceedings of the Conferences.

No publication of scientific paper is done in this Newsletter. We urge all the groups interested to submit a short text (one page maximum with photos eventually) on their research, their results or their projects, along with a list of references of their papers published during the past six months. This list will appear in the last item. Any information about meetings, conferences or others which we would not be aware of will be welcome.

Call for contributions to the newsletter

All issues of this newsletter are open for general contributions. If you would like to contribute any science highlight or workshop report, please contact Weitao Lyu (lyuwt@foxmail.com) preferably by e-mail as an attached word document.
The deadline for **2020 spring issue** of the newsletter is **May 15, 2020**.

PRESIDENT
Xiushu Qie
Chinese Academy of Sciences
E-mail: qiex@mail.iap.ac.cn

SECRETARY
Weitao Lyu
Chinese Academy of Meteorological Sciences
E-mail: lyuwt@foxmail.com

* The new website for ICAE, www.icae-iamas.org , is being constructed and will open soon.